BNL-105155-2014-TECH

Booster Technical Note No. 111;BNL-105155-2014-IR

Eddy current multipoles and sextupole configuration

G. F. Dell

February 1988

Collider Accelerator Department

Brookhaven National Laboratory

U.S. Department of Energy

USDOE Office of Science (SC)

DISCLAIMER

EDDY CURRENT MULTIPOLES AND SEXTUPOLE CONFIGURATION

AD

Booster Technical Note

No. 111

G. F. DELL

FEBRUARY 23, 1988

ACCELERATOR DEVELOPMENT DEPARTMENT

Brookhaven National Laboratory

Upton, N.Y. 11973

EDDY CURRENT MULTIPOLES AND SEXTUPOLE CONFIGURATION

G.F. Dell

Introduction

In the present report the effects on beam emittance produced by the placement of sextupoles used to correct chromaticity as well as effects of multipoles produced by eddy currents in the dipole vacuum chambers and from dipole saturation are considered. Throughout the report, the "reference" eddy current multipoles are those of Morgan and Kahn[1], generated for a B_{dot}=5 T/s at the proton injection field of B=1.56 kgauss. In Parts II and III, these multipoles have been scaled with B_{dot} and inversely with $B\rho$ to make them applicable throughout the accelerating cycle for both protons and heavy ions. In addition, multipoles arising from saturation (reported by Danby and Jackson[2]) have been used when considering heavy ion acceleration in Part III.

The horizontal and vertical chromaticities, CHX and CHY, are listed in Table I for the basic machine (Natural) and when the eddy current multipoles are included. The chromaticity changes produced by the eddy current sextupoles are listed in the column labelled ΔCH.

	Natural	Nat.+Eddy	ΔCH
CHX	-5.093	3.162	8.255
CHY	-5.447	-13.164	-7.717

Table I Chromaticities of the AGS Booster with and without eddy current sextupoles.

Previous tracking studies, for which the "reference" eddy current multipoles were used, showed a region around the natural chromaticity in which there was little emittance transfer between motion in the horizontal and vercal planes[3]. This is referred to as the "no coupling window"; See Figure 1. In the present study:

I. the shape of this window is investigated when the sextupole distribution is changed from the standard (1,2,4,7) scheme having sextupoles in half cells 1,2,4, and 7 to the (ALL) scheme having sextupoles in all half cells when the "reference" eddy current multipoles are present or absent. It is concluded that the distribution of chromaticity correcting sextupoles and not the eddy current multipoles are responsible for the no coupling window.

II. The strength of sextupoles required to correct the chromaticity to either zero or -5 during proton acceleration is determined for a realistic acceleration cycle.

III. Step II is repeated for the acceleration cycle anticipated for Au.

Multipoles

Eddy Currents-- The eddy current multipoles reported in Booster TN-4 were obtained using a vacuum chamber made of 304L stainless steel with a top and bottom 1.5 mm thick and a side wall 0.075" thick. The resistivity of 304L stainless is 8.09×10^{-7} ohm-m at 100 °C. For a B_{dot} of 5 T/s, the multipole coefficients relative to the injection field of 1560 gauss are:

	Multipoles
b_2	0.78×10^{0} m^{-2}
b_4	-2.4×10^{1} m^{-4}
b_6	-1.6×10^{3} m^{-6}

Table II Eddy current multipoles of Morgan and Kahn (Booster TN-4, "reference multipoles": B_{dot}= 5 T/s, B_0= 1.56 kG).

The vacuum chamber design now indicates the use of 316L stainless steel of 0.075 inch thickness throughout. The resistivity of 316L is 7.4×10^{-7} ohm-m at 100°C. The increased cross sectional area as well as the slightly reduced resistivity should increase the eddy currents by 20-25%.

In the present work, this difference has been ignored; instead, the effects produced by the time dependence of B_{dot} have been estimated by using B_{dot} from acceleration cycles suggested for protons[4] and heavy ions[5]. The linear scaling of b_2 with B_{dot} is described below:

Let $B_{dot}(0) = 5$ T/s, $B(0)=0.156$ T, and $b_2(0)=0.78$ m^{-2}.

1. Expand B(t) $\quad B(t)=B_0(t)+\Delta B_1(t)+\Delta B_2(t)+ \ldots = B_0(t)(1+b_1X+b_2X^2+\ldots)$
2. Consider the second order term. $\quad \Delta B_2(t)=B_0(t)b_2X^2$
3. Set X=1m, and find $b_2(t)$. $\quad b_2(t)=\Delta B_2(t)/B_0(t)$
4. Assume $\Delta B_2(t)$ is linear with B_{dot}. ($\Delta B_2(t)=(B_{dot}(t)/5)*\Delta B_2(0)$) $\quad b_2(t)=\frac{B_{dot}(t)}{5}*\frac{\Delta B_2(0)}{B_0(t)}$
5. Multiply by $B_0(0)\rho/B_0(0)\rho$ and set $\Delta B_2(0)/B_0(0)=b_2(0)$ $\quad b_2(t)=\frac{B_{dot}(t)}{5} * \frac{B_0(0)\rho}{B_0(t)\rho} * b_2(0)$
6. Set $B_0(0)\rho=2.149$, $b_2(0)=0.78$ $\quad b_2(t)=\frac{B_{dot}(t)}{B_0(t)\rho} * \frac{2.149}{5.0} * 0.78$ (1)

For a constant B_{dot}, the eddy currents should be independent of the magnet excitation; therefore the effective b_2 should vary inversely with $B_0(t)\rho$. In this note the question of the importance of eddy current multipoles (and therefore whether or not they require compensation) is addressed. This question is considered using more recent information on B_{dot} to scale the results reported in TN-4.

Saturation-- The dipole field reaches 12.75 kgauss during heavy ion acceleration, and sextupole effects due to magnet saturation contribute and become more important than than those due to eddy currents. The multipoles attributed to saturation are listed in Table III.

	B_o(kgauss)					
Mult	1.6	10.0	11.0	12.0	12.5	13.0
b_2	2.6E-3	-5.0E-2	-8.7E-2	-0.17	-0.24	-0.33
b_4	0.51	-9.73	-2.0E+1	-4.1E+1	-5.9E+1	-7.9E+1
b_6	4.1E+2	-1.2E+3	-3.3E+3	-6.1E+3	-7.4E+3	-7.8E+3
b_8	6.6E+5	-6.6E+5	0.0	0.0	0.0	0.0
b_{10}	0.0	0.0	0.0	0.0	0.0	0.0

Table III. Saturation multipoles of expressed as $b_n(m^{-n})$

Multipoles have been distributed over the length of each dipole according to Simpson's Rule. Each dipole is split in half; one-sixth of the multipole strength ($b_n*\ell/\rho$) is placed at each end of the dipole, and two-thirds is placed at the center. Only b_2 is included when determining the chromaticity (and therefore the strengths of sextupoles SF and SD). However, during tracking, all multipoles are included when evaluating the kick given to a test particle. In the following text, SF and SD are the names of the sextupoles, and S(f) and S(d) are used to indicate the strengths of SF and SD.

I. Chromaticity Window For No Coupling

Tracking results from a chromaticity scan of the AGS-Booster with the (1,2,4,7) sextupole configuration and eddy current multipoles indicate a sharp valley in which little emittance transfer occurs for chromaticities near the natural chromaticity[3]. The study was made using equal initial emittances in the horizontal and vertical planes, $\varepsilon_x=\varepsilon_y=50\pi$ mm mradians. During the scan, the chromaticity was incremented equally in both planes, and the maximum emittance in either plane was recorded. To determine the role of eddy current multipoles in determining the no coupling valley, two scans were made across the steepest portion of the valley ($-12.5\leq CH\leq 2.5$) when eddy current multipoles were present and then absent; the results are compared in Figure 2. There is a contribution to the emittance transfer caused by the eddy current multipoles, but this contribution only slightly alters the shape of the valley.

Additional scans were made to determine the dependence of the no coupling valley as well as the impact of the eddy current multipoles when the initial emittance of the particles was changed. These results are presented in Figure 3. They show the sharpness of the no coupling valley as well as the contribution from eddy current multipoles increases with beam emittance. As the

first order effect from sextupoles is quadratic in particle amplitude (and therefore linear with emittance), the roughly linear dependence on particle emittance is not surprising.

Two other tests were made to establish that the chromaticity sextupoles are responsible for the valley: a). the sextupole periodicity was increased to 24 (sextupoles in all half cells) to see if the valley changed, and b). the chromaticity sextupoles were removed by setting their strengths to zero.

a). Scans were made with and without eddy current multipoles. The results of these scans are shown in Figure 4 for a particle having equal initial emittances of 50π mm mradian in each plane. The scan reveals a broad valley in which the maximum emittance during a 600 turn tracking run increases by less than 10% as the chromaticity is varied by five units on each side of the minimum. Eddy current multipoles increase the valley floor by about 2% of the initial emittance, and they also caused a shift in the location of the minimum by 1.5 to 2 units. However, they do not determine the shape of the broad valley.

b). The strengths of the chromaticity correcting sextupoles were set to zero; the uncorrected lattice had a resulting horizontal chromaticity of 3.16 and a vertical chromaticity of -13.16. The maximum emittance during a 600 turn tracking run was 63.6π mm mradians ($\cong$27% emittance transfer). As this maximum emittance seemed small for such a large displacement from the center of the no coupling valley, a contour map plotting lines of equal maximum emittance was generated. This is presented in Figure 5 and reveals a long valley in which little emittance transfer takes place.

The desirability of having chromaticity correcting sextupoles in all half cells has been recognized for sometime, however there are certain half cells in which placement of special elements is thought to be incompatible with placement of sextupoles. In general, these are half cells 3 and 6 -- which have no dipoles. The use intended for these half cells is listed in Table IV. In addition to half cells 3 and 6, a conflict also occurs in half cells B8 (heavy ion kicker) and C5 (heavy ion kicker plus a foil).

Half cell	Element
A3	Empty
A6	rf cavity (protons)
B3	rf cavity (heavy ions)
B6	rf cavity (heavy ions)
C3	Electrostatic septum (heavy ions)
C6	HK (heavy ion kicker)
	PK (proton kicker)
	Damping system
D3	Dump kicker
D6	Dump septum
	Absorber block
E3	Tune meters
	Current transformer
E6	rf cavity (protons)
F3	Ejection kicker
F6	Ejection septum

Table IV List of special elements located in half cells 3 and 6.

Exploratory chromaticity scans were made with sextupole configurations intermediate between the (1,2,4,7) scheme and the (ALL) scheme. The first variation included sextupoles in all half cells but 3 and 6, the (1,2,4,5,7,8) scheme. The second variation, denoted as (1,2,4,5,7,8)*, varied from the first by having sextupoles absent in half cells B8 and C5. These two variations give results intermediate between the (1,2,4,7) and (ALL) schemes. The results, with and without eddy current multipoles are presented in Figure 6(a) for the (1,2,4,5,7,8) scheme and in Figure 6(b) for the (1,2,4,5,7,8)* scheme. The comparison of all four sextupole schemes at $\varepsilon_x=\varepsilon_y=50\pi$ with eddy current multipoles present are displayed in Figure 7. The evolution of the no coupling valley as the number of sextupoles is increased is clearly seen. The conclusion that sextupole configuration is responsible for the no coupling valley -- and conversely for the large emittance transfer and therefore large beam size off the center of the valley -- seems indisputable. Hence, it seems important to have a sextupole distribution that has a periodicity of 24 (sextupoles in all half cells).

II. Sextupole Strength Required for a Realistic Proton Acceleration Cycle.

The sextupole strength required for chromaticity correction has been determined for the proton acceleration cycle proposed by Cottingham[4]; see Figure 8 for the time dependence of B and Bdot. The time dependence of the eddy current multipole coefficients were obtained by using Eq-1. For convenience, a scale factor, Scale = $b_2(t)/0.78$, has been defined; this variable is used to express the linear dependence of the strengths of sextupoles, SF and SD, and the change of chromaticity on the effective b_2, see Figure 9. As mentioned previously, the effective b_2 is proportional to Bdot and inversely proportional to $B\rho$; the effective b_2 and $B(t)\rho$ are plotted in Figures 10(a) and 10(b), respectively. The increment of chromaticity contributed by the eddy current sextupoles during the acceleration cycle and the integrated sextupole strengths required to correct the chromaticity to zero are plotted on Figures 11(a) and 11(b), respectively.

The strengths S(f) and S(d) of sextupoles, SF and SD, evaluated by PATRICIA are independent of $B\rho$. They are related to the kick given to a particle by the expression (Appendix I):

$$X' = 0.5\ S\ X^2 = \Delta B_2\ \ell/(B\rho)\ ,$$

with S = S(f) or S(d). At X=1 m, the integrated sextupole field is:

$$\Delta B_2(t)\ell = 0.5\ S\ B(t)\rho \quad (T/m). \qquad (2)$$

Plots of $\Delta B_2\ell$ corresponding to the strengths of SF and SD from Figure 11(b) are shown on Figure 12. With the (1,2,4,7) sextupole scheme, an integrated field of $\Delta B_2\ell$ = -1.5 T/m for the focusing sextupoles and $\Delta B_2\ell$= 2.5 T/m for the defocusing sextupoles is required to correct the chromaticity to zero at the full proton energy.

As is seen from Figure 11(a), the increment of chromaticity due to eddy current sextupoles changes during the acceleration cycle. Were it not for the time dependence of chromaticity, the strengths of sextupoles SF and SD would be constant. This constant portion depends upon the final chromaticity; from

eq-2 it is seen that even though S(f) and S(d) are constant, $\Delta B2\ell$ varies with time. In the following discussion the $\Delta B2\ell$ necessary to correct the chromaticity to zero and to -5 is determined for the (1,2,4,7) and (ALL) sextupole schemes. For each scheme the strengths of SF and SD have a constant part that varies with desired chromaticity and a variable part that depends on the acceleration rate.

(1,2,4,7)	(CHX,CHY)	
S(f)= -0.64312 + SCALE * 0.4944 S(d)= 0.50424 + SCALE * 0.3286	(0,0)	(3a)
S(f)= -2.323E-2 + SCALE * 0.4944 S(d)= 3.326E-2 + SCALE * 0.3286	(-5,-5)	(3b)
(ALL)	**(CHX,CHY)**	
S(f)= -0.18218 + SCALE * 0.1424 S(d)= 0.29495 + SCALE * 0.1956	(0,0)	(3c)
S(f)= -6.532E-3 + SCALE * 0.1424 S(d)= 1.953E-2 + SCALE * 0.1956	(-5,-5)	(3d)

The time dependence of the chromaticity change depends upon the acceleration cycle and is the same for all for of the above cases. The time dependence of S(f) and S(d) for chromaticities (0,0) and (-5,-5) is plotted on Figure 13(a) for the (1,2,4,7) scheme, and the corresponding $\Delta B2\ell$ is plotted on Figure 13(b). It is seen that the largest requirement for sextupole strength arises from shifting the chromaticity away from its natural value. On Figure 14, the data of Figure 13(b) have been replotted on a different scale so they can be easily compared with the results obtained for the (ALL) scheme which are shown on Figure 15. Two general statements can be made: 1). the integrated sextupole field needed to correct the chromaticity to zero is approximately 2.5 times the strength required to correct it to -5, and 2). the integrated sextupole field required for the (1,2,4,7) scheme is approximately twice as large as that required for the (ALL) scheme.

III. Sextupole strength required for a realistic heavy ion cycle.

The analysis of section II has been repeated[5] for the heavy ion case. The acceleration cycle is that reported by Y.Y. Lee and is plotted in Figure 16. Equation 1 was used to determine the time dependence of the eddy current multipoles by scaling the "reference" multipoles linearly with Bdot and inversely with $B\rho$. At high fields the contribution from saturation was included; the time dependence of these saturation multipoles was estimated by plotting the data of Table III and using a relation, deduced from Figure 16, B(t)=1.38+0.025(t(ms)-40) kgauss as the time dependence of the magnetic field -- see Figure 17. The time dependence of b2 is shown on Figure 18; the peak results from Bdot reaching a constant value relatively early in the acceleration cycle; b2 for sulfur is enhanced by the lower magnetic field when Bdot reaches its maximum. The contribution to chromaticity is shown in Figure 19. The relations governing the strengths of SF and SD are the same as for the proton case (Eq -3). The required $\Delta B2\ell$ for the (1,2,4,7) and the (ALL) sextupole schemes are shown on Figures 20 and 21, respectively, for chromaticity correction to (0,0) and (-5,-5).

Discussion

From Part I it was established that the configuration of chromaticity correcting sextupoles, not the eddy current sextupoles, are responsible for the no coupling window, and conversely for the large transfer of emittance from one plane to the other for chromaticities far off the center of the valley.

For $\varepsilon_x=\varepsilon_y=50\pi$ and the (1,2,4,7) sextupole scheme, maximum emittances over 90π are observed when the chromaticity is ±5 units from the valley center (-5,-5). In contrast, the maximum emittance is less than 60π in this interval of chromaticity when the (ALL) scheme is used.

The strengths S(f) and S(d) of the chromaticity sextupoles SF and SD consist of a time dependent portion resulting from the time dependent eddy currents and a fixed part that is necessary to shift the chromaticity from its natural value to the value desired. For both protons and heavy ion acceleration, the b2 from eddy currents reaches its maximum relatively early in the accelerating cycle and then decreases by ≅50%. As the $\Delta B2\ell$ required is the product of $B\rho$ and the sextupole strength, the required integrated sextupole field depends more strongly on the desired chromaticity than upon the eddy currents.

The most demanding requirement is imposed during heavy ion acceleration where $B\rho$ may approaches 18 Tm. Additional requirements arising from magnet saturation indicate $\Delta B2\ell$=7.5 T/m for the (1,2,4,7) scheme and $\Delta B2\ell$=2.2 T/m for the (ALL) scheme when the chromaticity is to be corrected to zero. A listing of the maximum requirements for $\Delta B2\ell$ is given in Table IV.

		Protons		Heavy Ions*	
Scheme		0.0	-5	0.0	-5
(1,2,4,7)	SF	-1.4	+0.95	-7.5	-2.0
	SD	2.6	0.8	3.3	-1.0
(ALL)	SF	-0.4	0.28	-2.2	-0.55
	SD	1.5	0.48	1.9	-0.50

Table VI. Maximum $\Delta B2\ell$ (T/m) required for chromaticity correction. (* indicates inclusion of saturation multipoles.)

Only the study of Part I required tracking, and this was performed using "reference" multipoles. Inspection of Figures 10(a) and 18 reveals that b2(t) is most generally considerably less than the reference value of b2=0.78 m^{-2} and that b2(t) only barely reaches that value when Bdot first reaches its maximum, i.e. t=20.6 ms for protons and t=36 ms for heavy ions. Thus the impact of eddy current multipoles during proton and heavy ion acceleration would usually be less than that obtained in Part I and would equal the contribution seen in Part I for a relatively short part of the accelerating period. The conclusions of Part I indicate that sextupole configuration and not eddy current multipoles are responsible for the large emittance transfers observed in the tracking runs. The results of Parts II and III indicate the

influence of eddy current multipoles during proton and heavy ion acceleration is even less than that of Part I and further reduces the significance of these multipoles. Based on the present study, it is concluded that increasing the periodicity of the chromaticity sextupoles is important, while correcting the eddy current effects by using special coils on the vacuum chambers, is rather unimportant.

REFERENCES

1. G.Morgan and S. Kahn, Calculation of Eddy Currents in the Beam Tube, Booster TN-4 , January 28, 1986.
2. G. Danby and J. Jackson, Booster Dipole Field Computation,Booster TN-5 January 10, 1986.
3. G. Parzen, No Coupling Window in the Choice of Chromaticity in the AGS Booster, Booster TN-75, April 3, 1987.
4. J.G. Cottingham ,Proton Cycle for the Booster, Booster TN-49, July 2, 1986.
5. Y.Y. Lee, Heavy Ion Acceleration RF Program, Booster TN-52,July 10, 1986.

Appendix I

Verification of the relationship between kicks from sextupole elements and multipole elements.

The kick from a sextupole is: kick = 0.5 S X^2, where S is the sextupole strength determined by PATRICIA. The kick from a multipole is: kick = $b2\ell\ X^2/\rho$. Verify that, for equal kicks, $S = 2b2\ell/\rho$.

Method: The Booster lattice was modified so chromaticity sextupoles and multipole elements were placed at the center of all quadrupoles. A cell of the modified lattice follows:

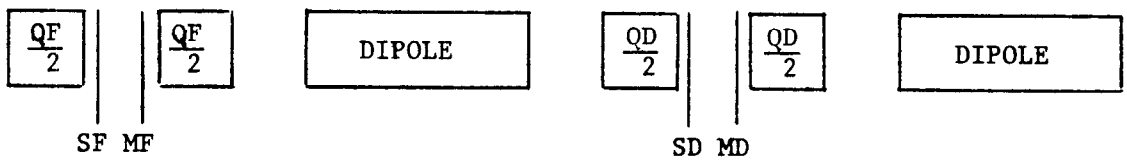

Figure: Altered Booster cell used to establish the relationship between the strengths of sextupoles (SF and SD) and the strengths of multipoles (MF and MD).

The strengths of the sextupoles were evaluated when b2 = 1 m^{-2} was placed at element MF in the QF's and then at element MD in the QD's. The results are shown in the following Table.

b2(MF)	b2(MD)	S(f)	S(d)	ΔS(f)	ΔS(d)
0.0	0.0	-0.13444	0.24747		
1.0	0.0	-0.06144	0.24747	-0.0700	0.00
0.0	1.0	-0.13444	0.17447	0.0	0.0700

Table A: ΔS(f) and ΔS(d) produced by b2 = 1 m^{-2} in QF's or QD's.

From above, $S = 2\ b2\ell/\rho$. Runs were made for ℓ/ρ=0.0365. S = 0.0700 is predicted and agrees with the measurement in the table above. Hence, the relation is verified.

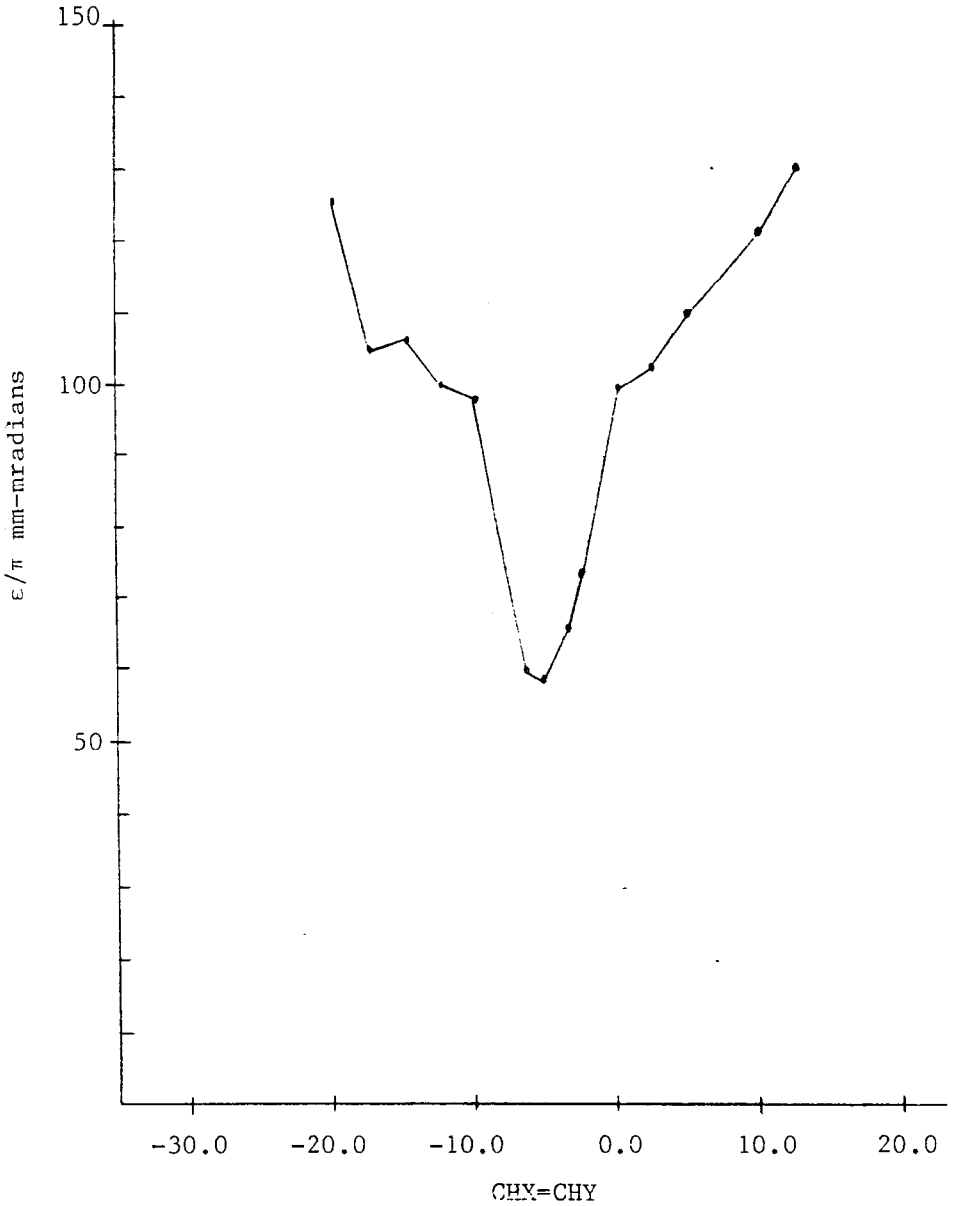

Figure 1. Chromaticity scan showing the maximum emittance of a particle in either plane during 600 turn tracking runs. Initial conditions: ν_x=4.820, ν_y=4.830, $\varepsilon_x=\varepsilon_y=50\pi$ mm mradians, (1,2,4,7) sextupole scheme, "reference" eddy current multipoles.

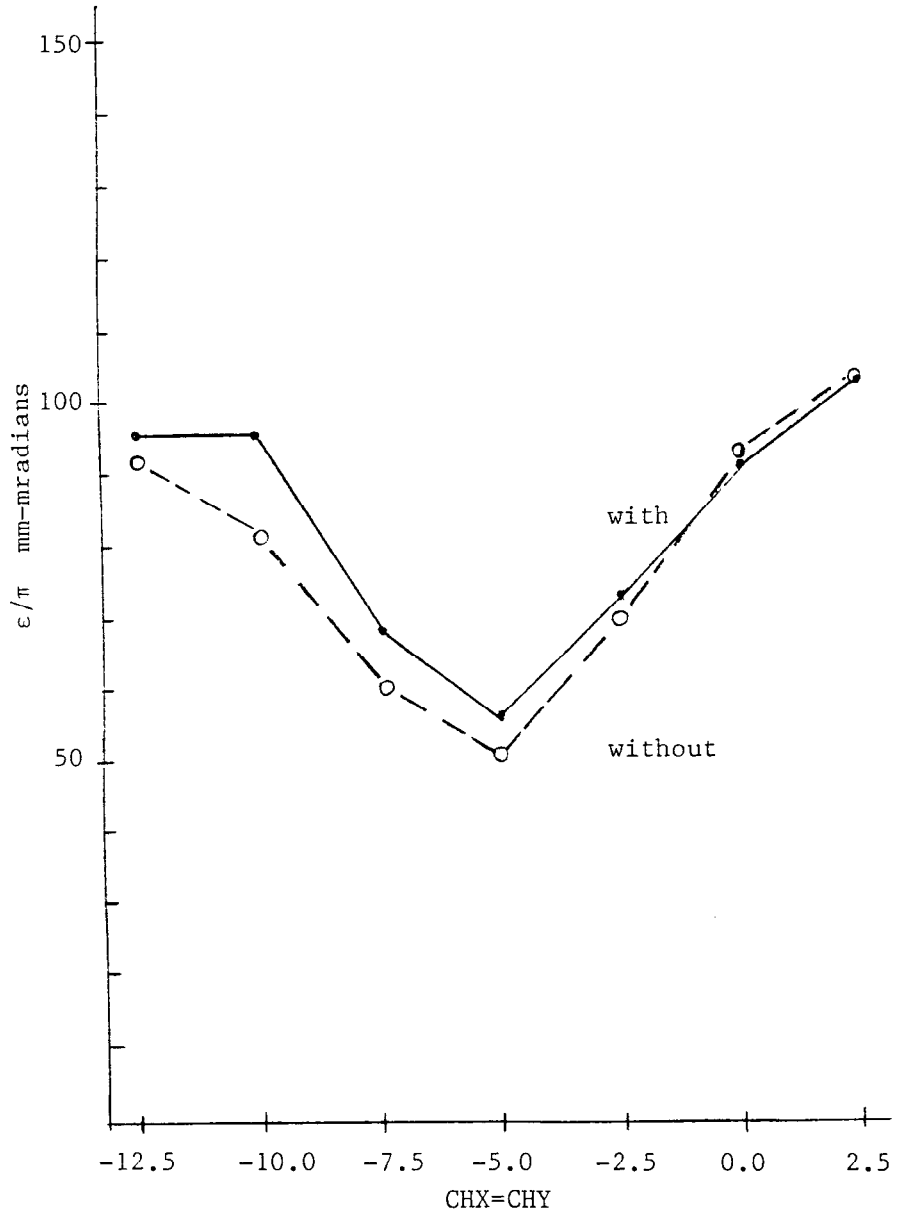

Figure 2. Chromaticity scan, (1,2,4,7) sextupole scheme, with and without eddy current multipoles. The eddy current multipoles increase the emittance transfer, but they do not determine the shape of the no coupling valley.

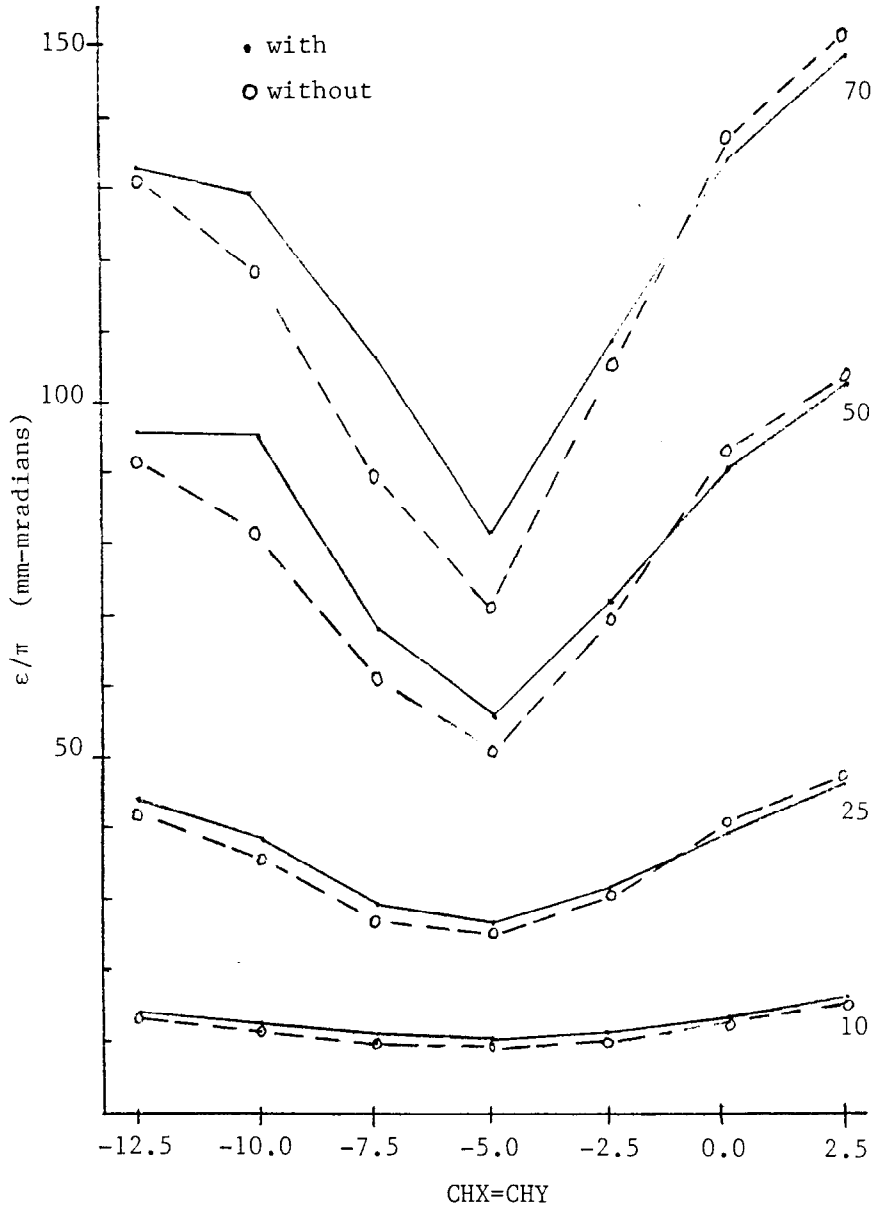

Figure 3. Chromaticity scans for the (1,2,4,7) sextupole scheme showing the valley profile as a function of the initial emittance of the particle when eddy current multipoles are present or absent. $\varepsilon_x=\varepsilon_y=10\pi$, 25π, 50π, or 70π mm-mrad. Both the sharpness of the valley and the contribution from eddy current multipoles increases with particle emittance.

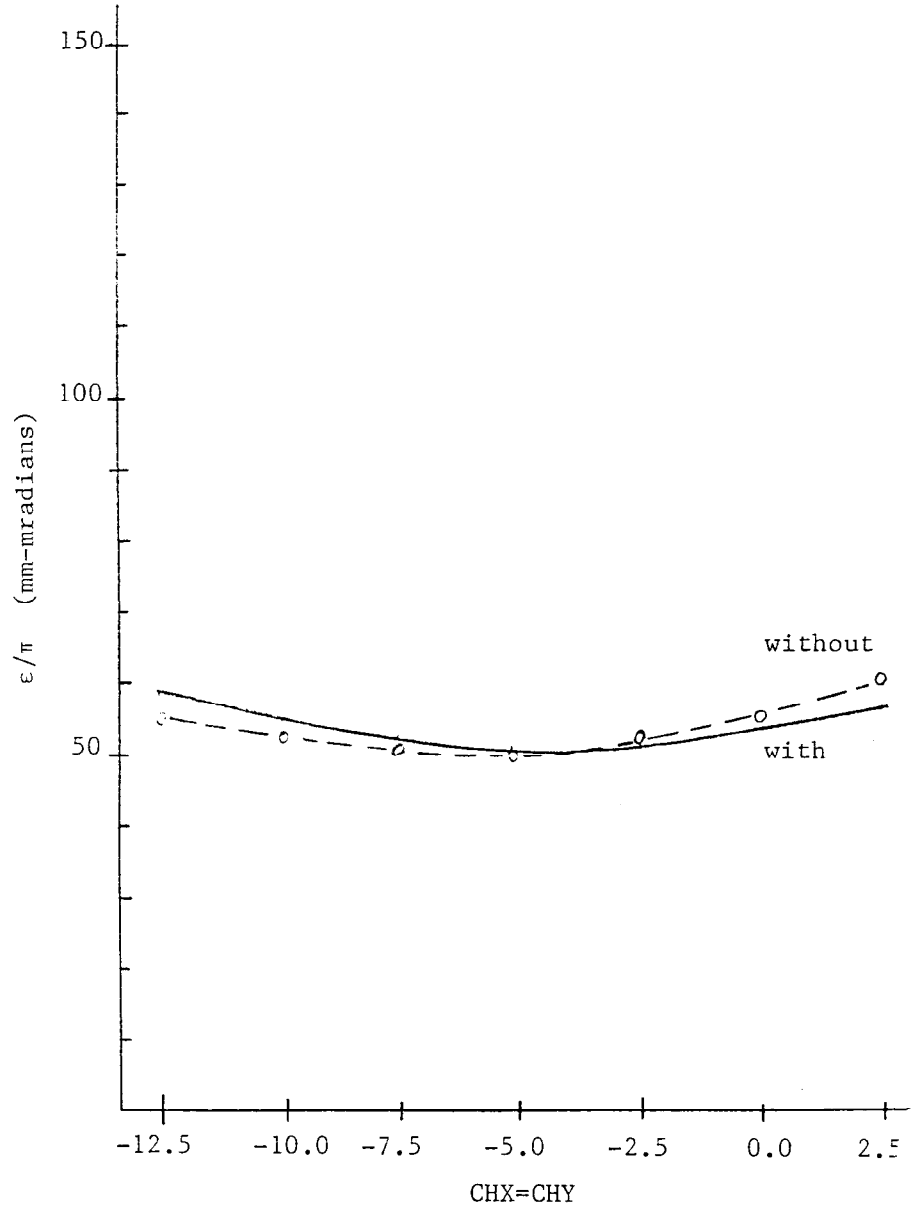

Figure 4. Chromaticity scan for the (ALL) sextupole scheme, with and without eddy current multipoles, when $\varepsilon_x=\varepsilon_y=50$ π mm mradians. Eddy current multipoles shift the center of the valley but only increase the valley floor by 1π (2%).

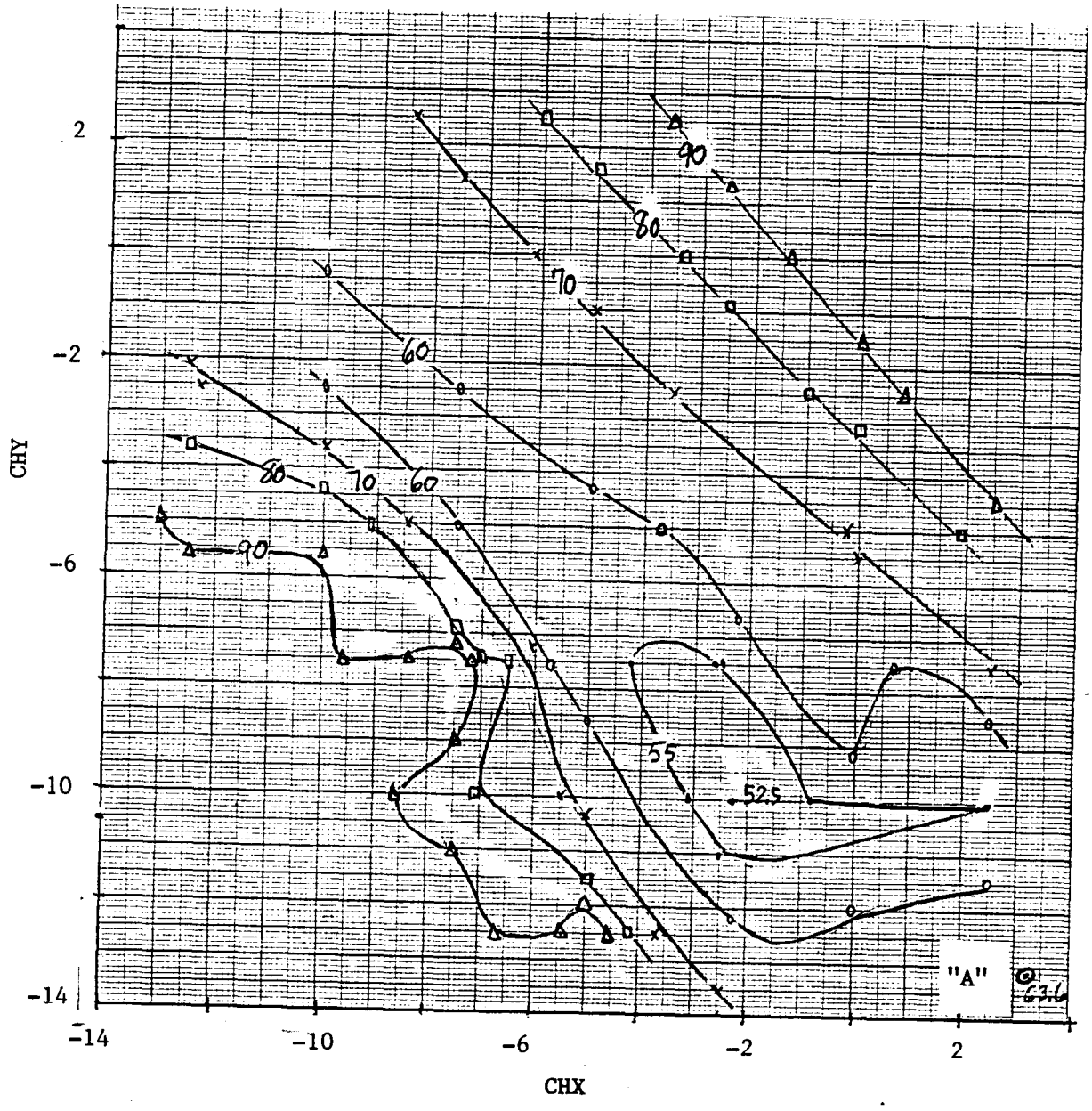

Figure 5. Contour map showing lines of equal emittance for a scan with $\varepsilon_x=\varepsilon_y=50\pi$ mm mradians for the (1,2,4,7) sextupole scheme. The maximum emittance for four paticles, (X,Y)≠0, (X,Y')≠0, (X',Y)≠0, and (X',Y')≠0, is plotted. Valley profiles in previous figures correspond to the diagonal with CHX=CHY. Point "A" denotes the maximum emittance when CHX=3.162 and CHY=-13.164. (S(f)=S(d)=0.0).

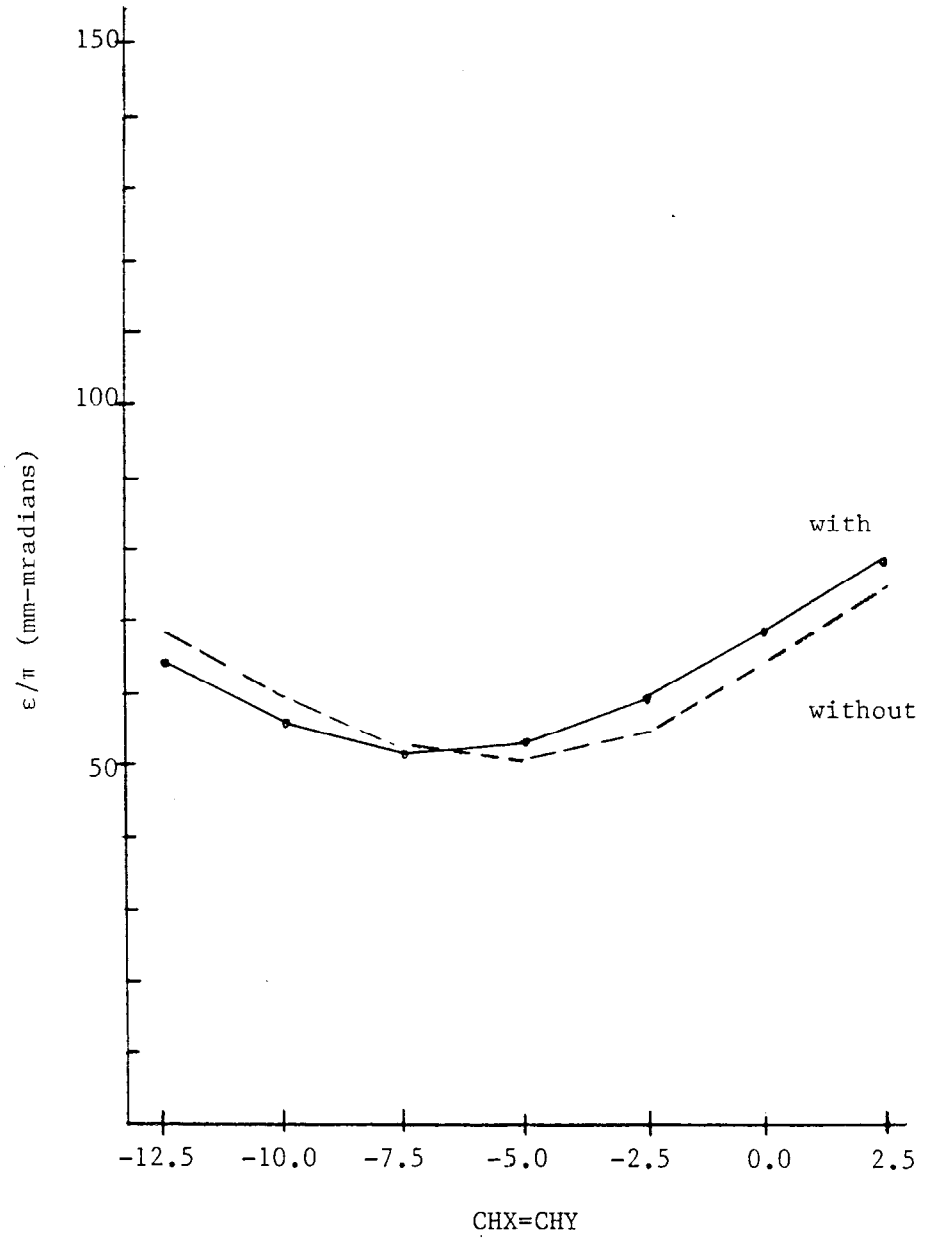

Figure 6(a). Chromaticity scan for the (1,2,4,5,7,8) sextupole scheme (Chromaticity sextupoles in all half cells but 3 and 6). $\varepsilon_x=\varepsilon_y=50\pi$ mm mrad. Scans were made with and without eddy current multipoles. The valley shape is basically unaltered by eddy current multipoles.

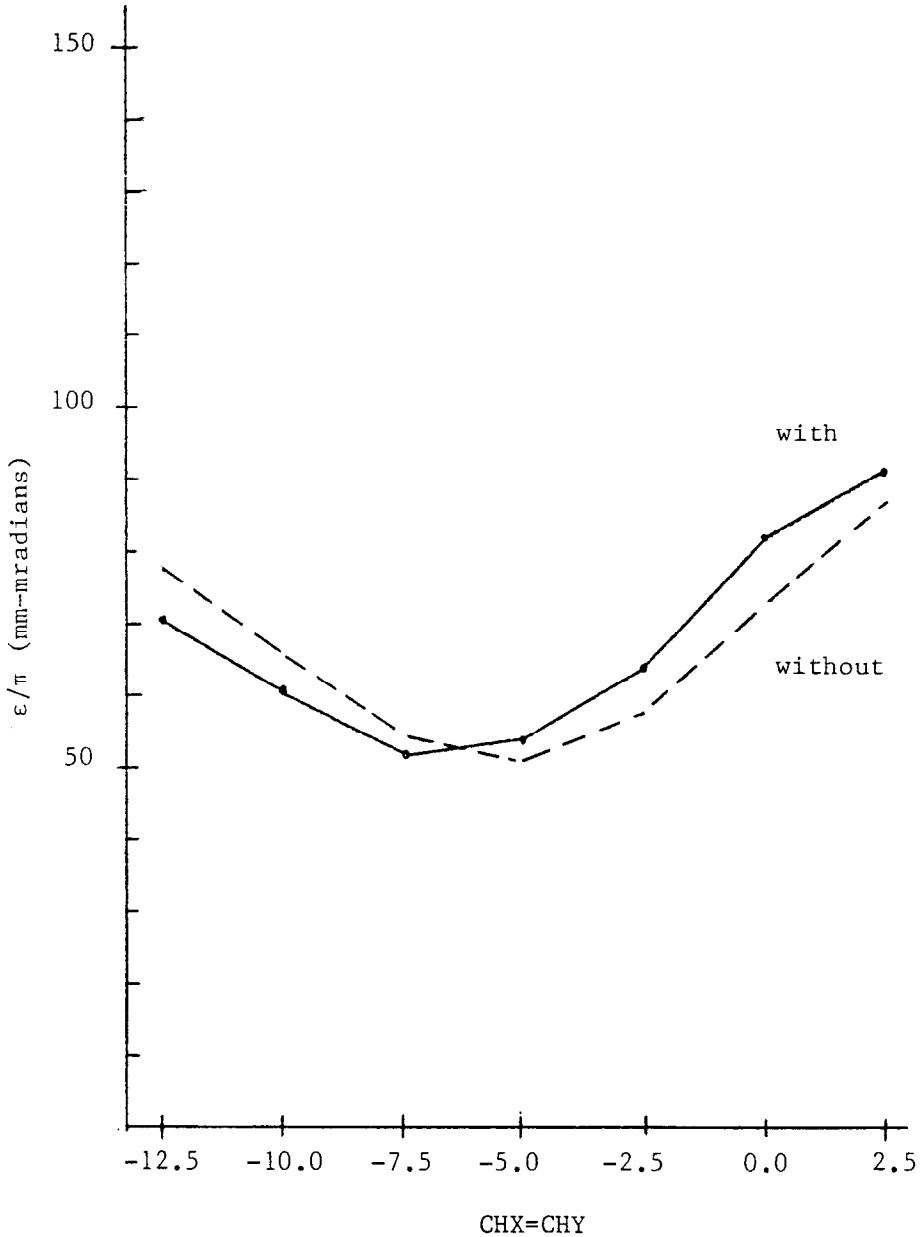

Figure 6(b). Chromaticity scans for the (1,2,4,5,7,8)* sextupole scheme. Sextupole scheme differs from that of Figure 6(a) in that sextupole SD is absent in half cell B8 and sextupole SF is absent in half cell C5. Scans made with and without eddy current multipoles at $\varepsilon_x=\varepsilon_y=50\ \pi$ mm mrad. The valley shape is basically unaltered by eddy current multipoles.

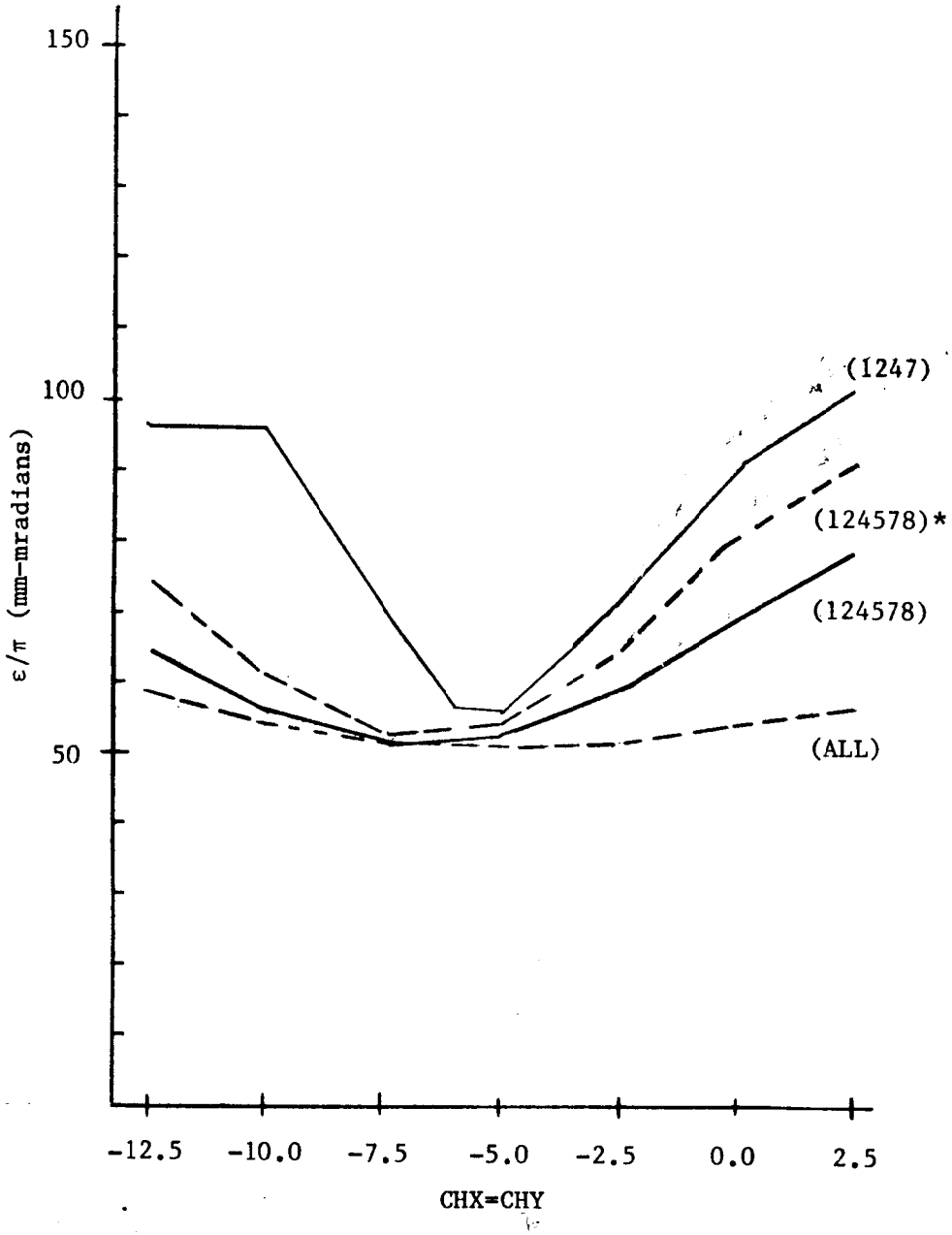

Figure 7. Comparison of four sextupole schemes showing the evolution of the no coupling valley as the sextupole schemes progress from the (ALL) scheme to the (1,2,4,7) scheme. Eddy current multipoles are present and $\varepsilon_x=\varepsilon_y=50\pi$ mm mrad.

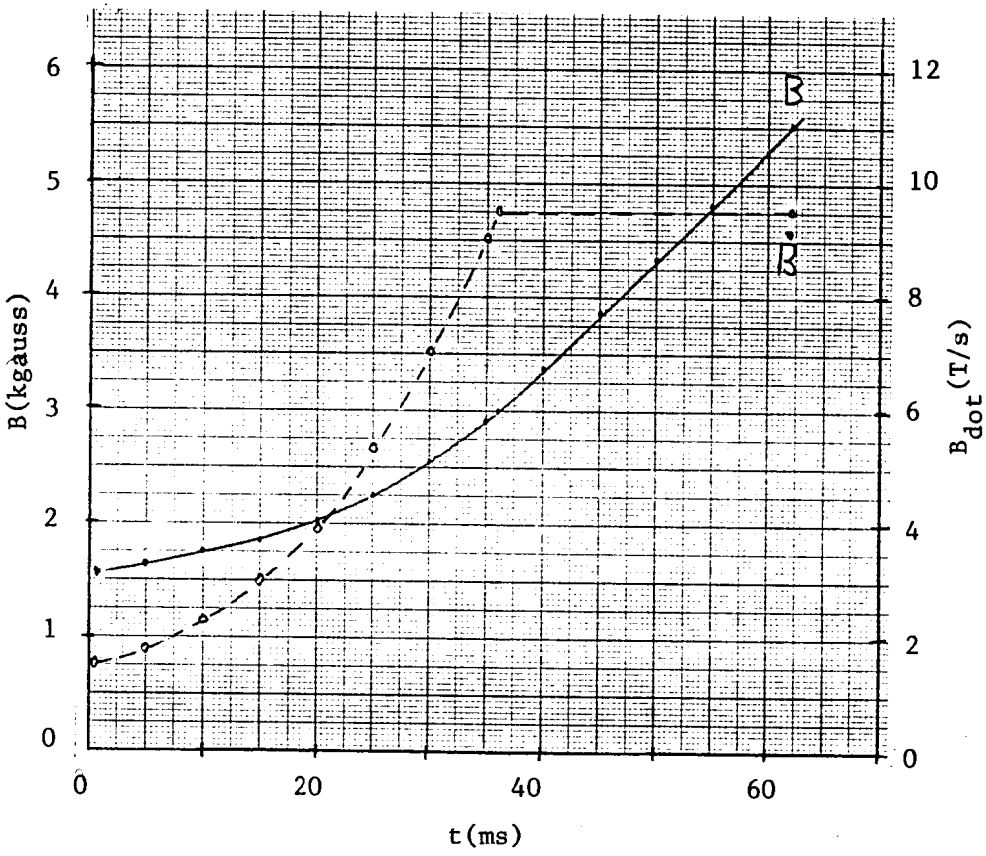

Figure 8. Time dependence of B(t) and $B_{dot}(t)$ for the proton cycle used by Cottingham in Booster TN-49. Maximum B_{dot}=9.5 T/s. Cycle length is 62 ms.

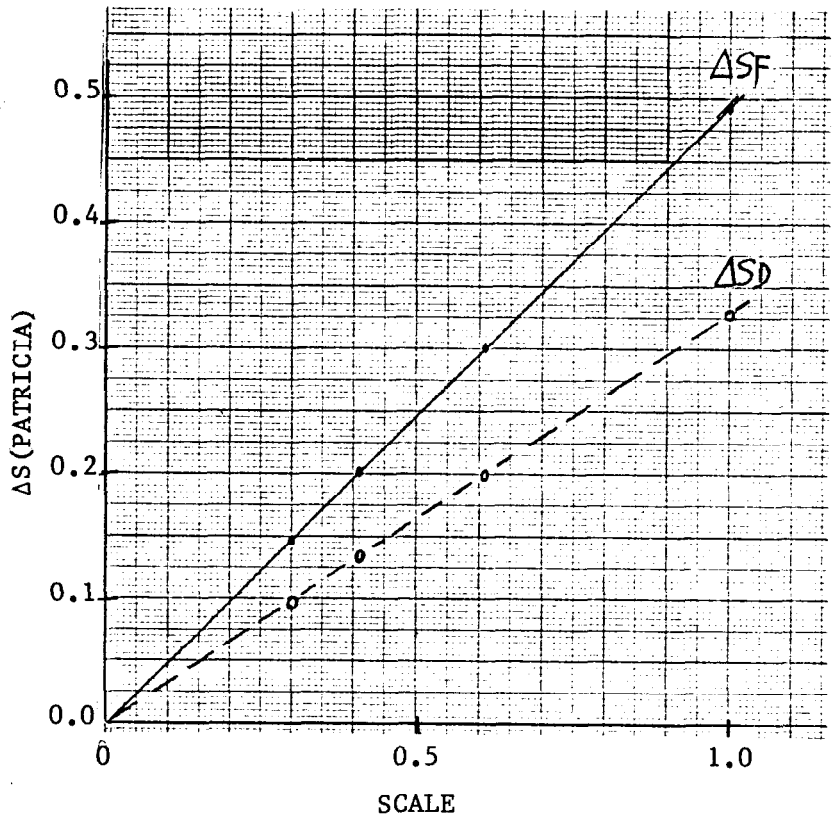

Figure 9(a). Increment of sextupole strength, (1,2,4,7) scheme, required to correct the chromaticity to zero as the eddy current multipoles are varied between zero and their reference values. b_2=SCALE*0.78 m^{-2}.

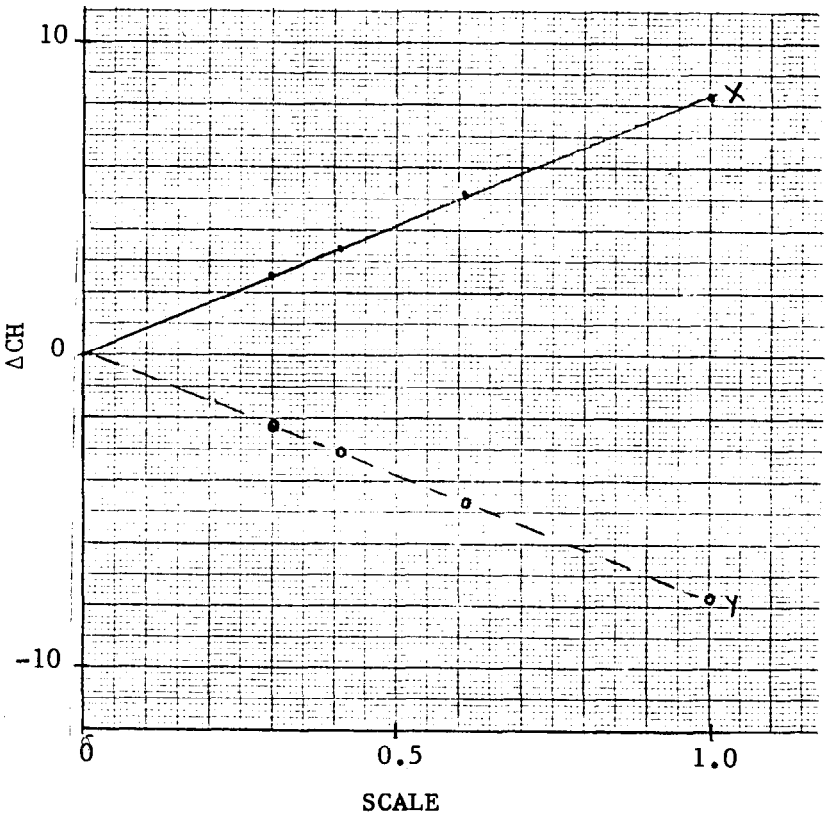

Figure 9(b). Chromaticity change as the eddy current multipoles are scaled between zero and their reference values. b_2=SCALE* 0.78 m^{-2}.

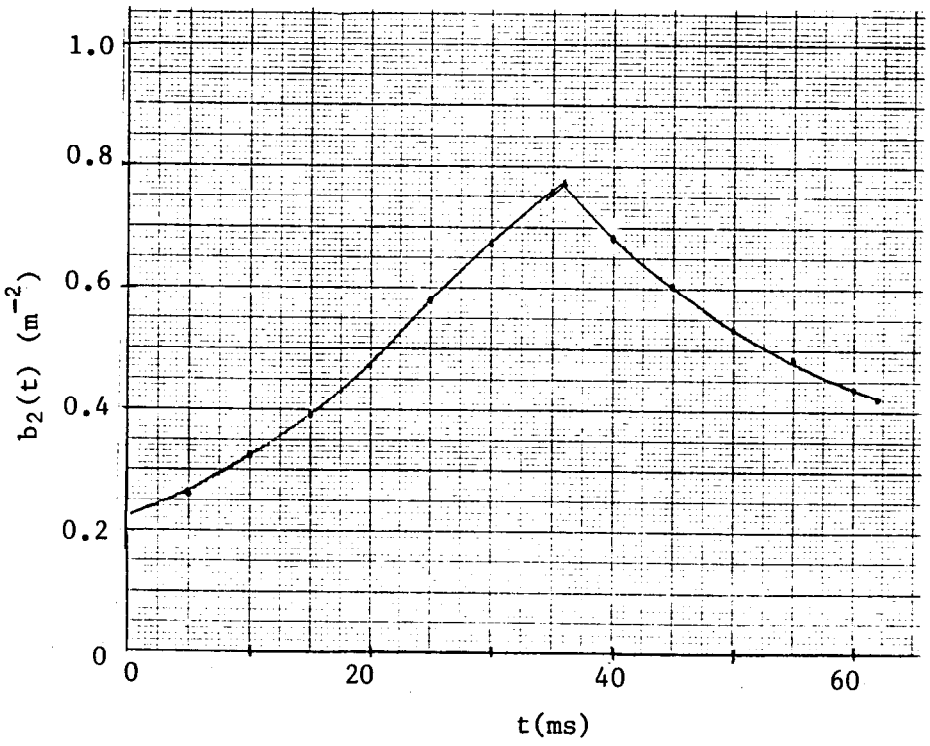

Figure 10(a). Time dependence of the eddy current sextupole coefficient $b_2(t)$ during the acceleration cycle of Figure 8. The reference eddy current sextupole has been scaled with $B_{dot}(t)$ and $B(t)\rho$ using Eq-1.

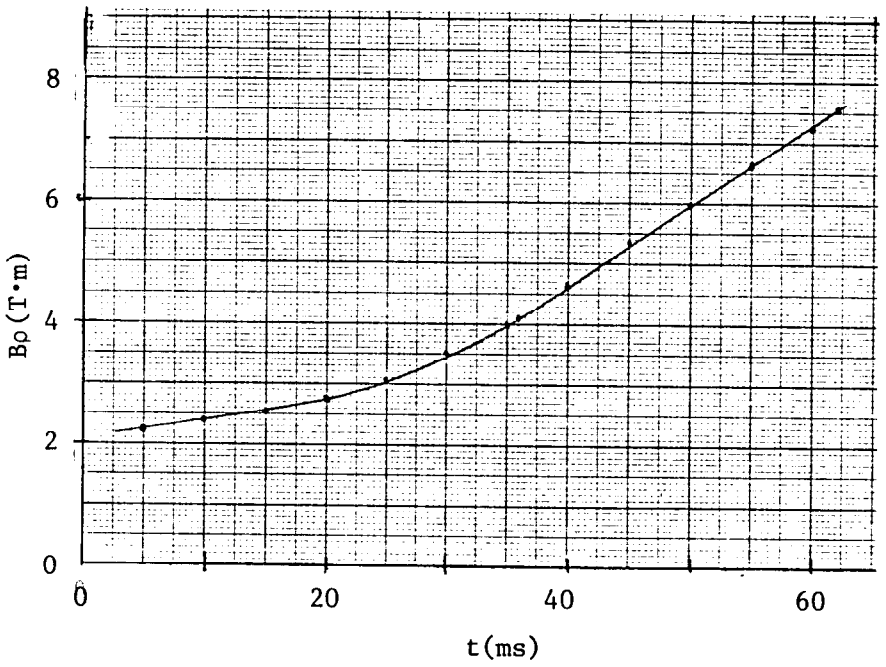

Figure 10(b). Time dependence of $B(t)\rho$ during the proton acceleration cycle.

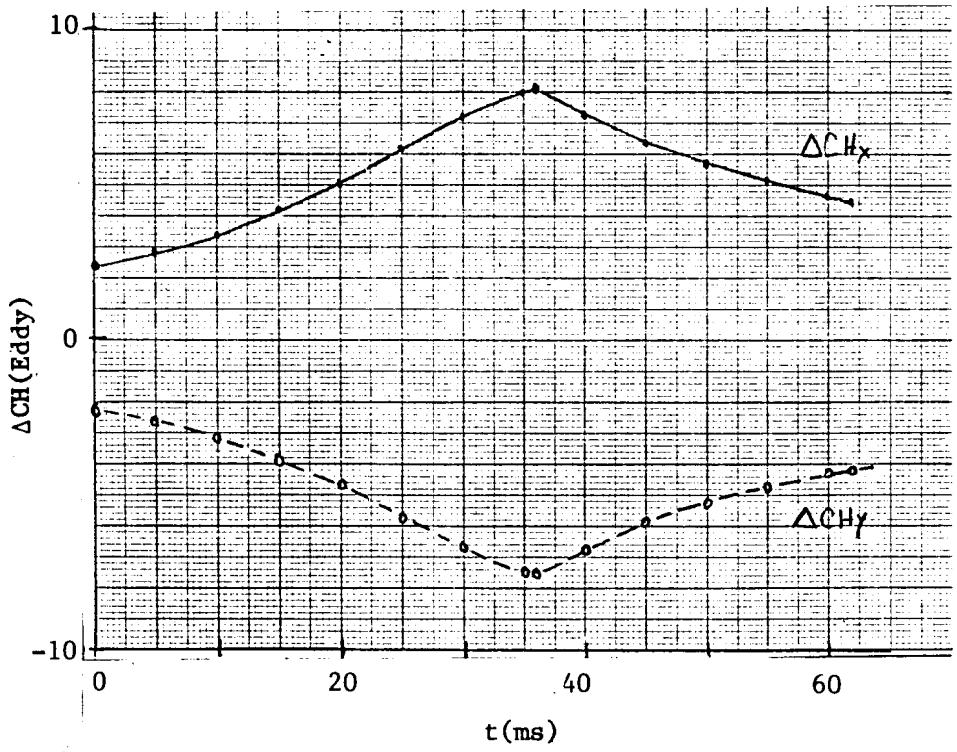

Figure 11(a). Time dependence of the chromaticity change, induced by the eddy current sextupole of Figure 10(a), during the proton acceleration cycle.

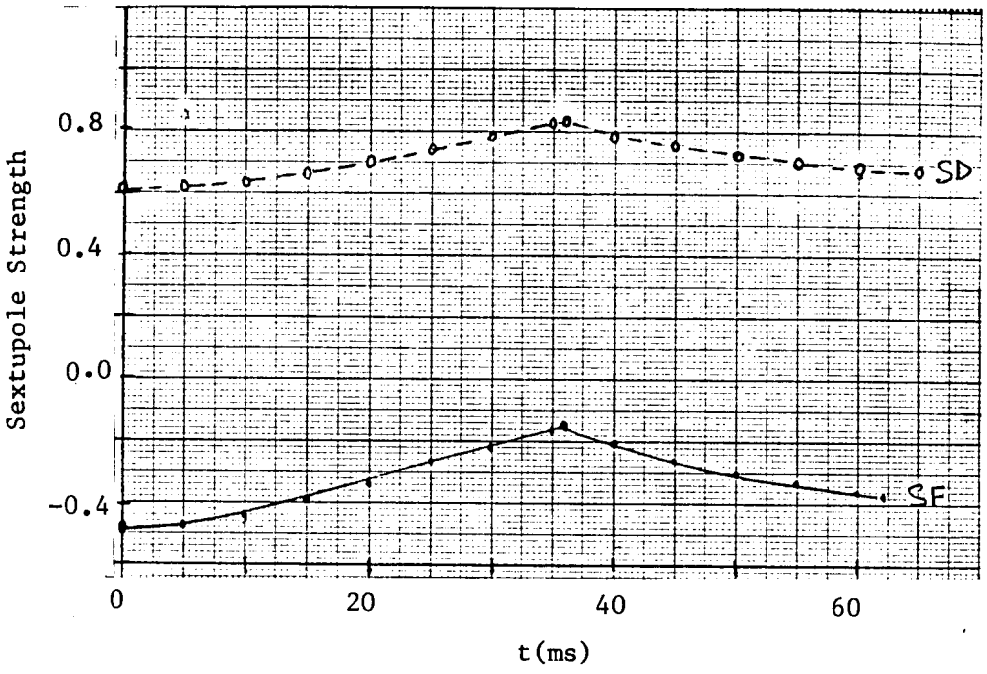

Figure 11(b). Time dependence of the strengths S(f) and S(d) of sextupoles SF and SD needed to correct the chromaticity to zero with the sextupole scheme (1,2,4,7) and eddy current multipoles.

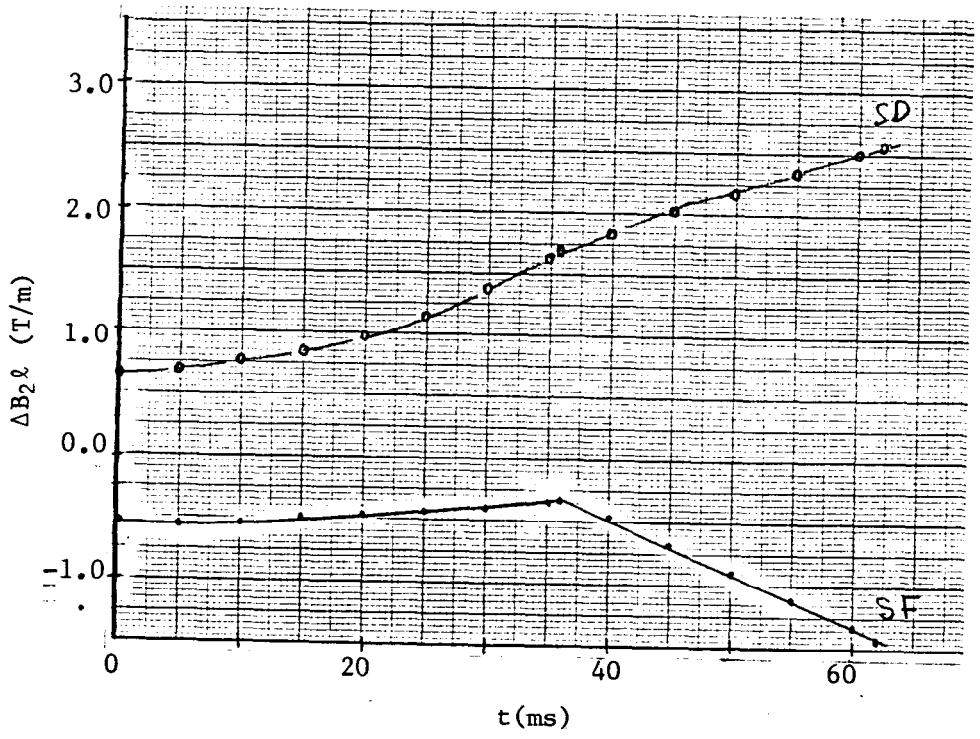

Figure 12. Time dependence of the integrated sextupole field $\Delta B_2 \ell$ needed to correct the chromaticity to zero with the (1,2,4,7) sextupole scheme.

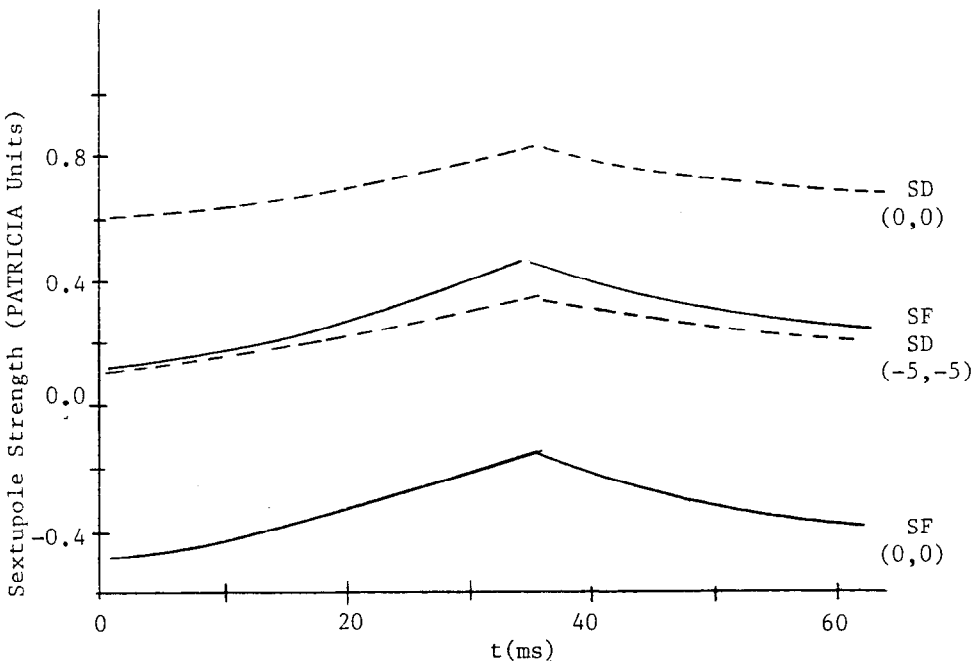

Figure 13(a). Time dependence of S(f) and S(d) needed to correct the chromaticity to zero and (-5,-5) with the (1,2,4,7) sextupole scheme when eddy current multipoles are present.

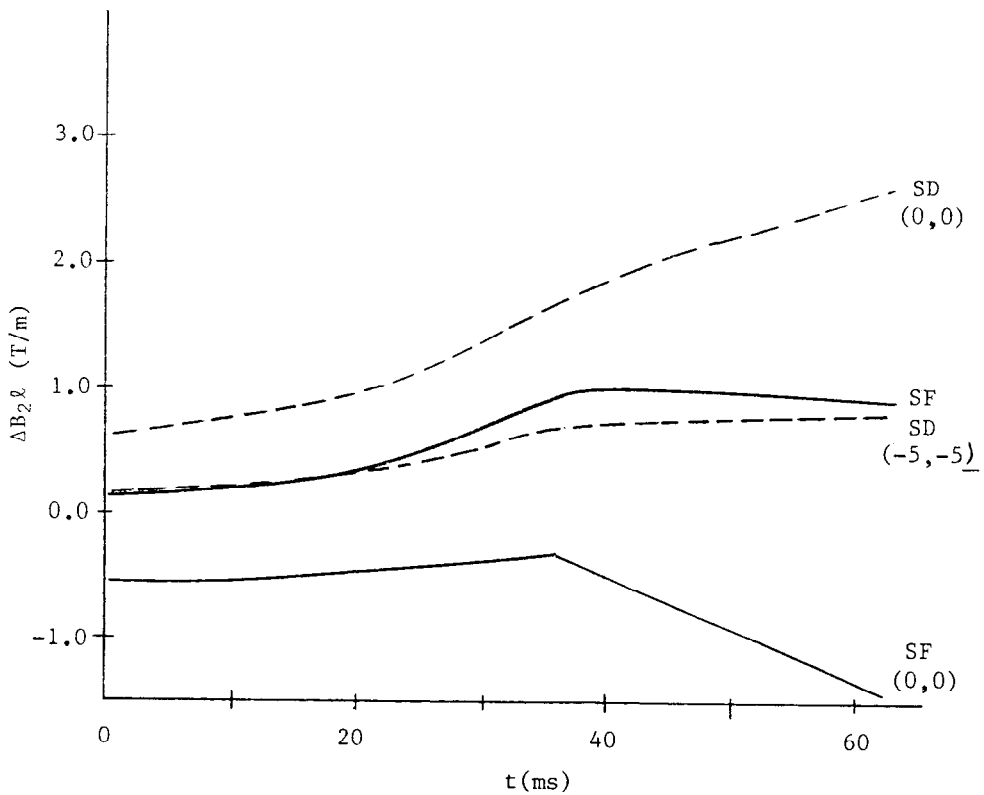

Figure 13(b). Time dependence of $\Delta B2\ell$ of sextupoles SF and SD needed to correct the chromaticity to zero and -5 with the (1,2,4,7) sextupole scheme.

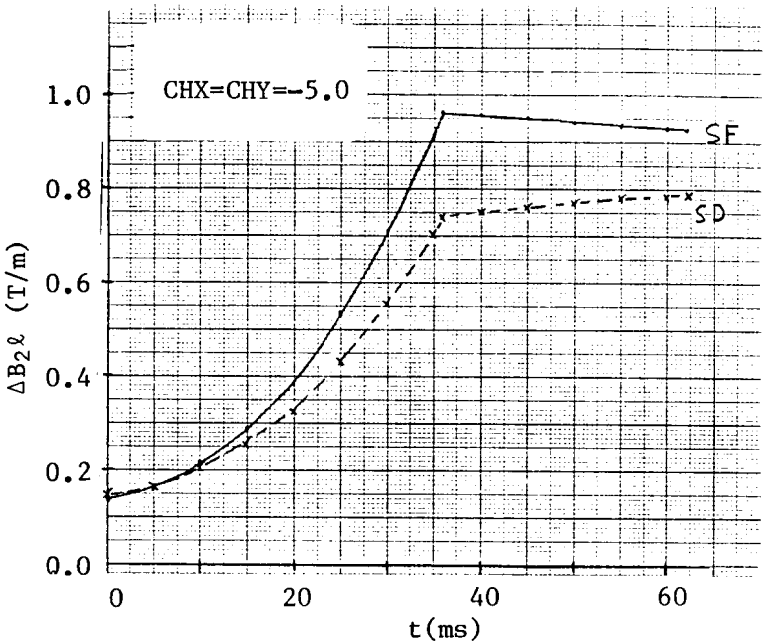

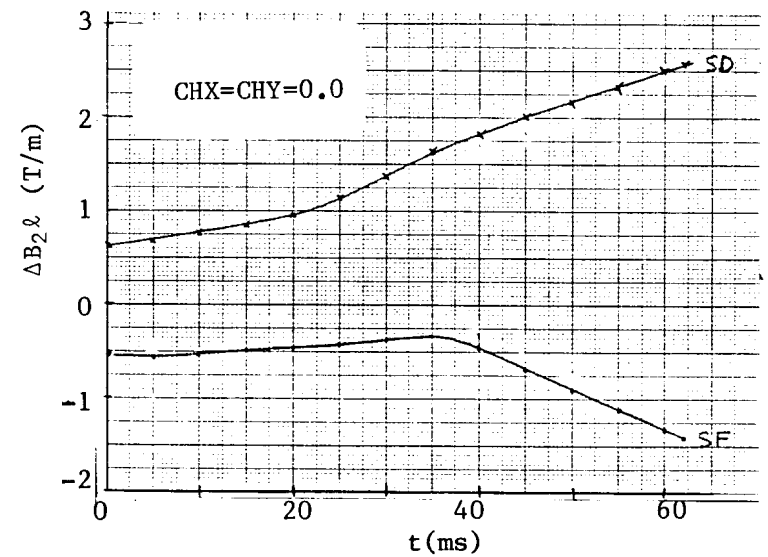

Figure 14. Replot of the data from Figure 13(b) showing the time dependence of $\Delta B2\ell$ for chromaticity correction with the (1,2,4,7) sextupole scheme. Data has been replotted to ease comparison with Figure 15.

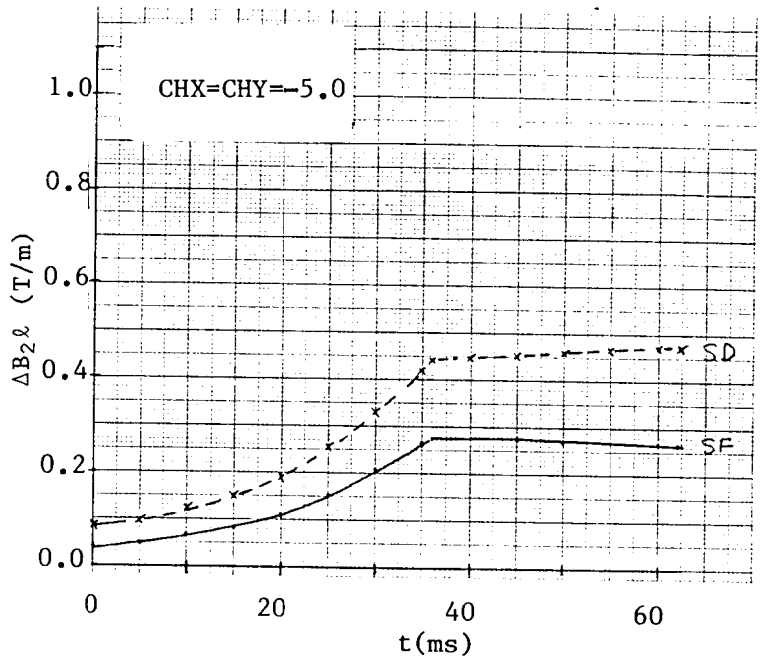

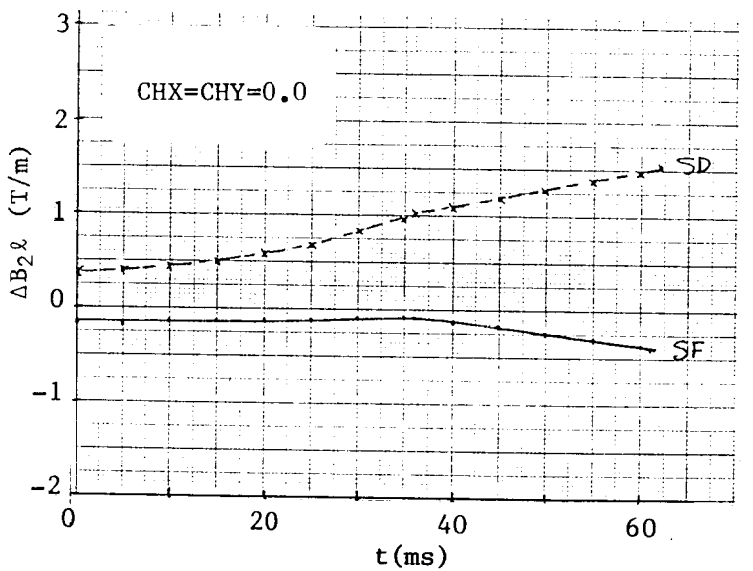

Figure 15. Time dependence of $\Delta B2\ell$ needed to correct the chromaticity to zero and to -5 using the (ALL) sextupole scheme. The integrated strength is approximately half that required with the (1,2,4,7) scheme.

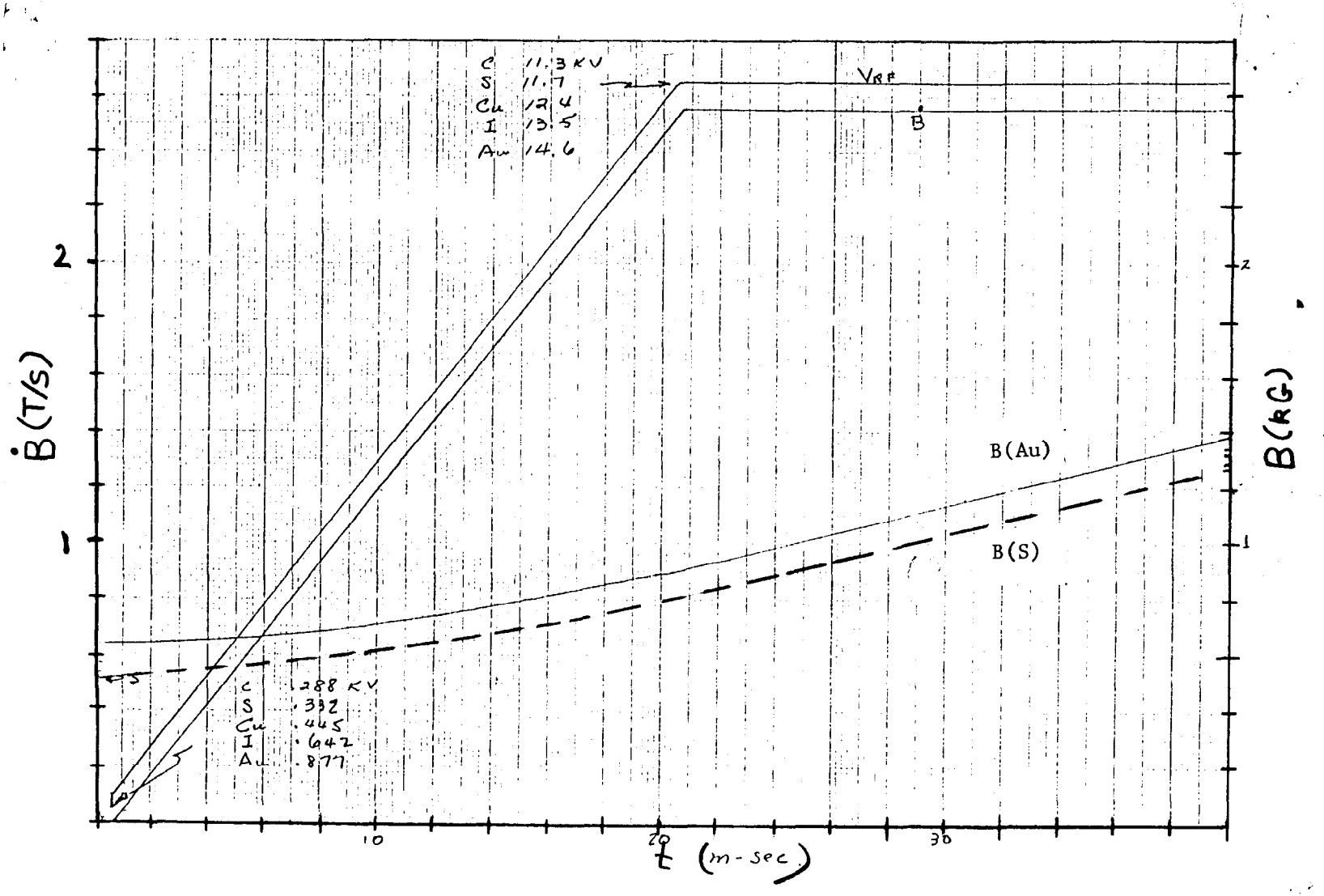

Figure 16. Time dependence of B(t) and $B_{dot}(t)$ for the heavy ion cycle used by Y.Y. Lee in Booster TN-52. $B_{dot}(t)$ reaches its maximum of 2.55 T/s after 20.6 ms and remains constant throughout the rest of the 500 ms acceleration period. The solid B(t) curve represents Au, and the dashed curve represents sulphur. B(t) for sulfur is less than that for Au and results in a larger b_2 for the same B_{dot}-- see Figure 18.

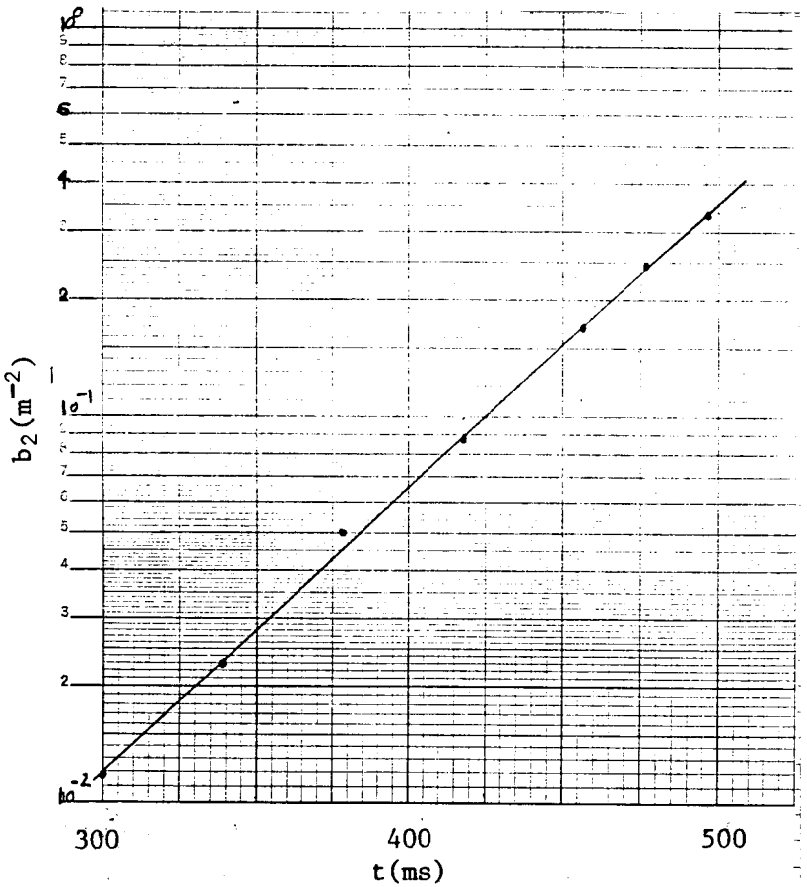

Figure 17. Time dependence of the saturation b2 obtained from the dependence of b2 on B(t) of Table III and the time dependence of B(t) deduced from Figure 16: B(t)=1.38 + 0.0255(t(ms)-40) with B in kgauss and t in ms.

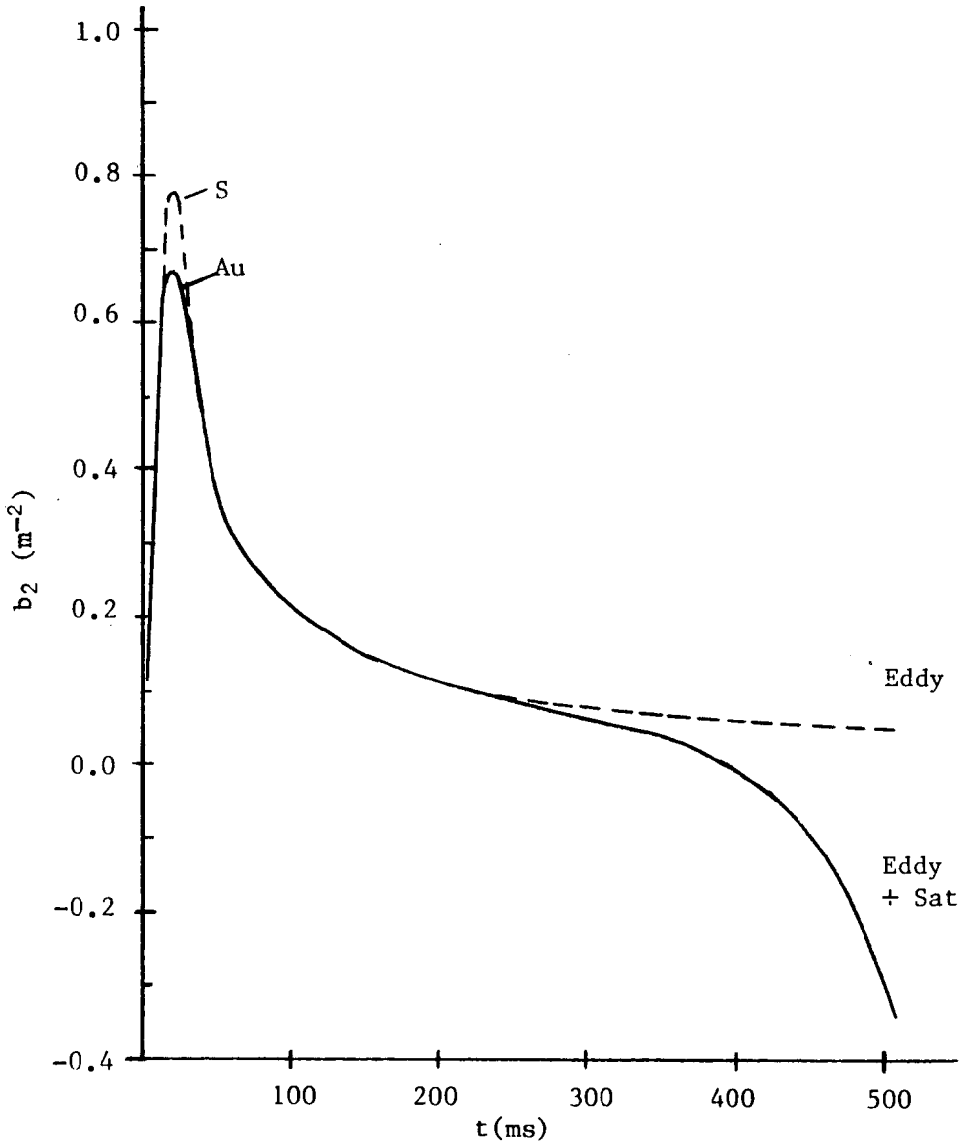

Figure 18. Time dependence of b2 for Au and S. Dashed curve for t≥300 ms indicates eddy current multipoles only; solid curve for t≥300 indicates net b2 from eddy currents plus saturation.

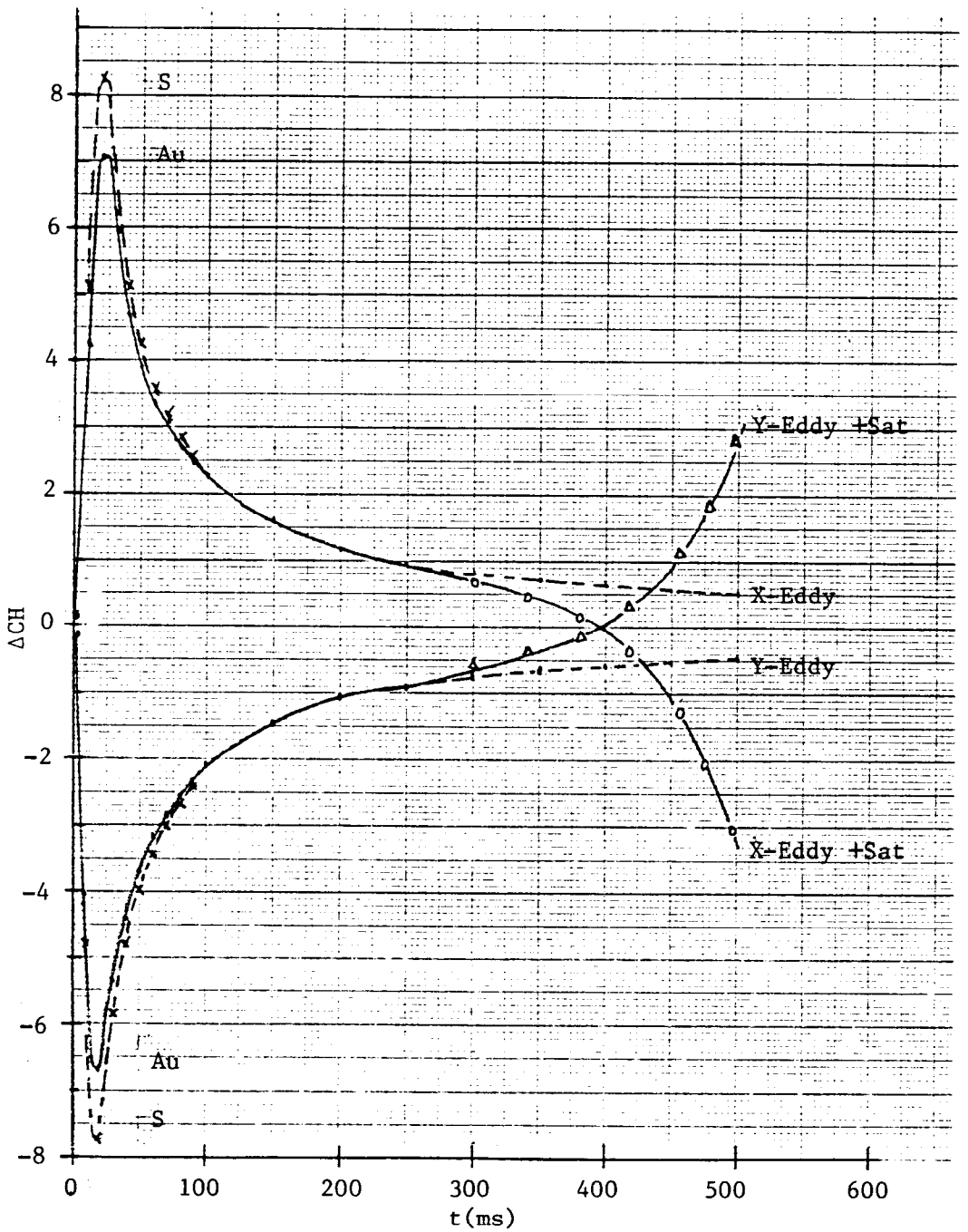

Figure 19. Time dependence of the chromaticity change produced by eddy current multipoles plus iron saturation. For t≥300 ms, dashed curve in-dicates eddy current multipoles only and solid curve indicates eddy currents plus saturation effects.

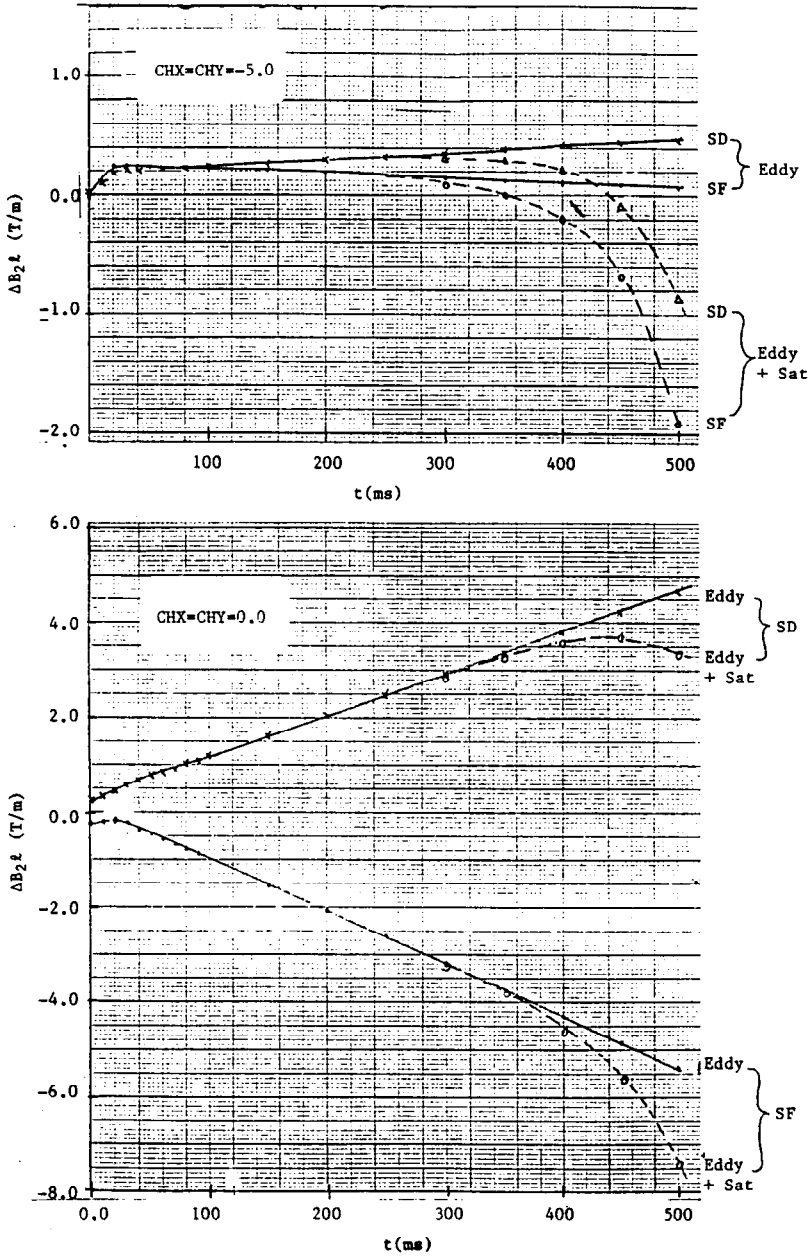

Figure 20. Time dependence of the integrated sextupole field $\Delta B2\ell$ for the chromaticity corrected to zero and -5 with the (1,2,4,7) sextupole scheme. For t≥300 ms, the effects with eddy currents only and with eddy currents plus saturation are shown.

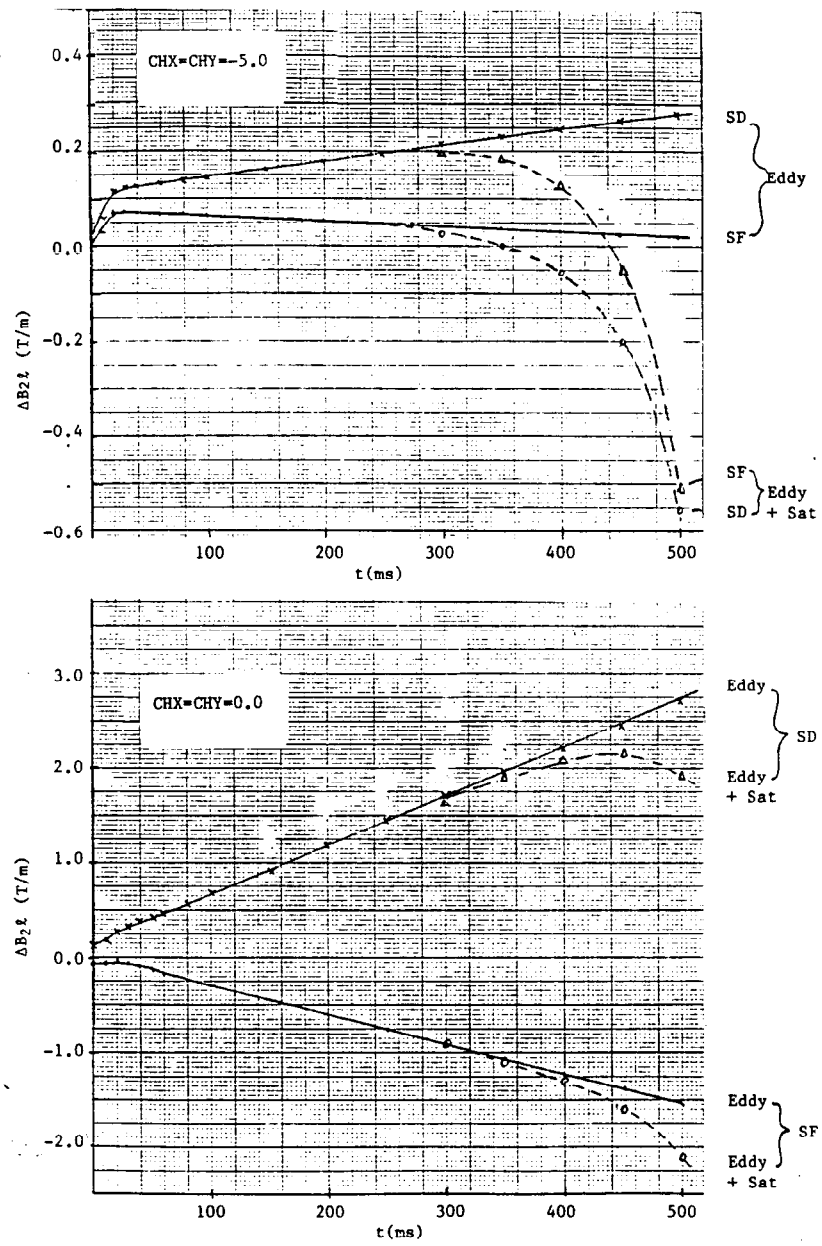

Figure 21. Time dependence of the integrated sextupole field $\Delta B2\ell$ needed to correct the chromaticity to zero and -5 with the (ALL) sextupole scheme. For t≥300 ms, the effects of eddy currents only and the from eddy currents plus sextupoles are shown.